Sub-micrometric reflectometry for localized label-free biosensing

R. Casquel,[1,2] J.A. Soler,[3] M. Holgado,[1,4*] A. López,[4] A. Lavín,[1,2] J. de Vicente,[1] F.J. Sanza,[4] M.F. Laguna,[1,4] M.J. Bañuls,[5] and R. Puchades[5]

[1]*Department of Applied Physics. Escuela Superior de Ingenieros Industriales. Universidad Politécnica de Madrid, C/José Gutiérrez Abascal,2, 28006, Madrid, Spain*

[2]*Laser Centre. Universidad Politécnica de Madrid. Carretera de Valencia km 7.300, 28031 Madrid, Spain*

[3]*Universidad Carlos III. Department of Bioengineering and Aerospace Engineering. Escuela Politécnica Superior, Avd. de la Universidad, 30. 28911 Leganés, Madrid, Spain*

[4]*Centre for Biomedical Technology. Universidad Politécnica de Madrid. Campus de Montegancedo. Pozuelo de Alarcón, 28223Madrid, Spain*

[5]*Instituto de Reconocimiento Molecular, Departamento de Química, Universidad Politécnica de Valencia, Camino de Vera s/n, 46022 Valencia, Spain*

[*]*m.holgado@upm.es*

Abstract: In this work we present an optical technique for characterizing sub-micrometric areas based on reflectivity of the light as a function of angle of incidence for the two pure polarizations s and p, covering a range of angles of incidence from −71.80° to 71.80° with a resolution of 0.1°. Circular areas with a diameter in the order of 600 nm can be characterized, and the spectra for the two polarizations can be obtained with a single measurement. For biosensing purposes, we have fabricated several Bio Photonic Sensing Cells (BICELLs) consisting of interferometers of 1240 nm of SU-8 polymer over silicon. An indirect immunoassay is performed over these BICELLs and compared experimentally with FT-VIS-NIR spectrometry and theoretical calculations. The Limit of Detection (LoD) achieved is comparable with standard high resolution spectrometry, but with the capability of analyzing sub-micrometric domains for immunoassays reactions onto a sensing surface.

OCIS codes: (280.4788) Optical sensing and sensors; (310.6860) Thin films, optical properties.

References and links

1. X. Fan, I. M. White, S. I. Shopova, H. Zhu, J. D. Suter, and Y. Sun, "Sensitive optical biosensors for unlabeled targets: A review," Anal. Chim. Acta **620**(1-2), 8–26 (2008).
2. J. Homola, "Surface plasmon resonance sensors for detection of chemical and biological species," Chem. Rev. **108**(2), 462–493 (2008).
3. C. A. Barrios, M. J. Bañuls, V. González-Pedro, K. B. Gylfason, B. Sánchez, A. Griol, A. Maquieira, H. Sohlström, M. Holgado, and R. Casquel, "Label-free optical biosensing with slot-waveguides," Opt. Lett. **33**(7), 708–710 (2008).
4. M. C. Estevez, M. Alvarez, and L. M. Lechuga, "Integrated optical devices for lab-on-a-chip biosensing applications," Laser Photonics Rev. **6**(4), 463–487 (2012).
5. A. J. Haes and R. P. Van Duyne, "A nanoscale optical biosensor: Sensitivity and selectivity of an approach based on the localized surface plasmon resonance spectroscopy of triangular silver nanoparticles," J. Am. Chem. Soc. **124**(35), 10596–10604 (2002).
6. V. Kugel and H. Ji, "Nanopillars for sensing," J. Nanosci. Nanotechnol. **14**(9), 6469–6477 (2014).
7. M. Holgado, C. A. Barrios, F. J. Ortega, F. J. Sanza, R. Casquel, M. F. Laguna, M. J. Bañuls, D. López-Romero, R. Puchades, and A. Maquieira, "Label-free biosensing by means of periodic lattices of high aspect ratio SU-8 nano-pillars," Biosens. Bioelectron. **25**(12), 2553–2558 (2010).
8. M. Holgado, R. Casquel, B. Sánchez, C. Molpeceres, M. Morales, and J. L. Ocaña, "Optical characterization of extremely small volumes of liquid in sub-micro-holes by simultaneous reflectivity, ellipsometry and spectrometry," Opt. Express **15**(20), 13318–13329 (2007).
9. http://www.n-eos.com/
10. A. Rosencwaig, J. Opsal, D. L. Willenborg, S. M. Kelso, and J. T. Fanton, "Beam profile reflectometry: A new technique for dielectric film measurements," Appl. Phys. Lett. **60**(11), 1301 (1992).

#235177 - $15.00 USD Received 24 Feb 2015; revised 27 Mar 2015; accepted 6 Apr 2015; published 4 May 2015

11. J. T. Fanton, J. Opsal, D. L. Willenborg, S. M. Kelso, and A. Rosencwaig, "Multiparameter measurements of thin films using beam-profile reflectometry," J. Appl. Phys. **73**(11), 7035–7040 (1993).
12. J. M. Leng, J. Chen, J. Fanton, M. Senko, K. Ritz, and J. Opsal, "Characterization of titanium nitride (TiN) films on various substrates using spectrophotometry, beam profile reflectometry, beam profile ellipsometry and spectroscopic beam profile ellipsometry," Thin Solid Films **313–314**, 308–313 (1998).
13. C. Dainty, *Laser Speckle and Related Phenomena*, (Springer Verlag, 1984).
14. R. Casquel, *Biosensors Based on Vertically Interrogated Optofluidic Sensing Cells*. Doctoral thesis (Universidad Politénica de Madrid, 2012).
15. F. J. Sanza, M. F. Laguna, R. Casquel, M. Holgado, C. A. Barrios, F. J. Ortega, D. López-Romero, J. J. García-Ballesteros, M. J. Bañuls, A. Maquieira, and R. Puchades, "Cost-effective SU-8 micro-structures by DUV excimer laser lithography for label-free biosensing," Appl. Surf. Sci. **257**(12), 5403–5407 (2011).
16. GUM, Guide to the Expression of Uncertainty in Measurement. Available online: http://www.bipm.org/en/publications/guides/gum.html
17. H. P. Ho, W. C. Law, S. Y. Wu, C. Lin, and S. K. Kong, "Real-time optical biosensor based on differential phase measurement of surface plasmon resonance," Biosens. Bioelectron. **20**(10), 2177–2180 (2005).

1. Introduction

The use of optical devices for label-free biosensing has been extensively reported during past years [1]. In a general term, sensors are characterized either by measuring the reflectivity or transmissivity as a function of wavelength or angle of incidence of the light source, being sensors based on Surface Plasmon Resonance [2] and interferometric devices [3] two of the most studied typologies. Since the sensing surfaces are being reduced, due to the achievements on micro-nanofabrication techniques applied to biosensors and lab-on-a-chip devices [4], there is an interest in developing optical techniques able to characterize an area as small as possible. There are examples of the progress in this direction: for localized surface plasmon resonance sensors [5], which measure the change in resonance using nanoparticles with sizes in the order of 100 nm, or for sensing nanopillars of different materials [6,7], with diameters of several hundred of nanometers.

In a previous work [8] we reported the optical characterization of volumes of several fluids with increasing refractive indexes, filling a periodic array of conical sub-micrometric holes, with a total volume in the order of 0.3 fL each hole. In this work we report an evolution of this optical interrogation technique, which the measurement of reflectivity as a function of angle of incidence and with a variety of polarization states, and which has a sub-micrometric spot (in the order of 0.6 μm), achieved by using a high numerical aperture microscope objective (NA = 0.95). Furthermore, it is used a high resolution CCD camera, which provides an angular resolution of 0.1° and even lower helping in achieving a competitive limit of detection of the sensing system.

For analyzing the properties of this optical system applied to the field of label-free biosensing, we have measured several Biophotonic Sensing Cells (BICELLs [7]), consisting of an array of Fabry-Perot interferometers of 1240 nm of SU-8 polymer over silicon. The SU-8 sensing surface is biofunctionalized with Bovine Serum Albumin (BSA), and an immunoassay is performed for several increasing concentrations to recognize its corresponding antibody (antiBSA), measuring the reflectivity for s and p polarizations, and also measuring reflectivity as a function of wavelength with an FT-VIS-NIR high resolution spectrometer. Finally we have compared the experimental results with theoretical calculations, using a vertical film stack analytical model.

2. Experimental setup

The schematic of the optical layout is shown in Fig. 1. There are two different light sources, a laser diode emitting at 637 nm and a white light bulb, and two different cameras (a color camera and a high resolution monochromatic camera). The white light and the color camera are used for positioning and for focusing samples; the laser source is the core of the optical technique; the optical path of the light includes several expander and lenses, and a 150x objective to focus on the sample (L6). The position of the laser beam on the BICELL can be changed by moving a X-Y stage.

#235177 - $15.00 USD Received 24 Feb 2015; revised 27 Mar 2015; accepted 6 Apr 2015; published 4 May 2015

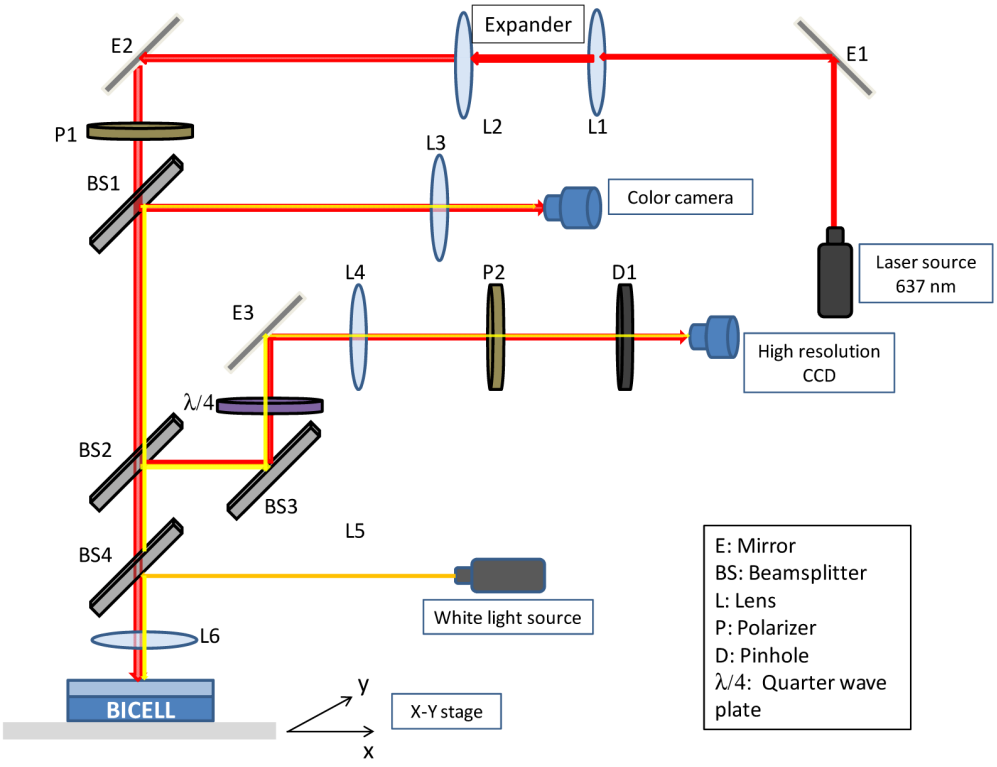

Fig. 1. Schematic of the optical setup. In this technique a polarized laser beam is focused (with the converging lens L6) on the BICELL and in the way back it passes through the same converging lens (L6), a quarter-wave plate (l/4), another converging lens (L4), an analyzer (P2), and then the intensity of the beam intensity is captured on a high resolution CCD. The data registered on the CCD is then displayed on a computer screen, showing an interference pattern (Fig. 3). The system have also a color camera used for positioning the laser beam in the BICELL within the x-y stage.

The laser beam focuses on the sample through a Leica 150x objective, with a Numerical Aperture (NA) of 0.95. The reflected beam goes through several beam splitters (BS4, BS2 and BS3), and then pass through a quarter wave plate, before being collected by a high resolution CCD camera. This optical characterization technique, that we call Reflectometry at Profile Level (RPL), was developed in collaboration with Nightingale EOS [9], and it is a variation of two former techniques, Beam Profile Reflectometry and Beam Profile Ellipsometry [10–12]. The more remarkable characteristics are that the system collects the reflectivity of a variety of angles of incidence and polarization states with a single measurement, and with a sub-micrometric spot size. The main improvements of RPL compared with the system based on Beam Profile Reflectometry and Ellipsometry used in our previous work are introducing a high resolution CCD camera instead linear arrays, which allows collecting mixed polarized states and improving resolution, and the use of a 150x objective, instead a 100x, reducing the spot size. Following the Rayleigh criterion, for a wavelength of 637 nm and a numerical aperture of 0.95, the diffraction limit is in the order of 550 nm.

$$d \simeq 0.82 \cdot \frac{\lambda}{NA} \tag{1}$$

The measuring principle is illustrated in Fig. 2. The basic concept is that a coherent light beam, in this case a laser beam focused through a high numerical aperture (N.A.) microscope

#235177 - $15.00 USD Received 24 Feb 2015; revised 27 Mar 2015; accepted 6 Apr 2015; published 4 May 2015

objective can be divided in light rays that focus on the sample surface with angles ranging from 0° to $\sin^{-1}$(NA), with a correspondence of the angle of incidence with the distance of a particular ray to the centre of the beam. In this case, using an objective with N.A. of 0.95 the angles range from 0 to 71.80°. With the proper use of an array detector of a number *n* of pixels, there is a direct correspondence between each pixel and a particular angle of incidence. The use of the lambda quarter plate and the polarizer is used in Beam Profile Ellipsometry, but does not affect the polarization state of pure s and p polarized beams.

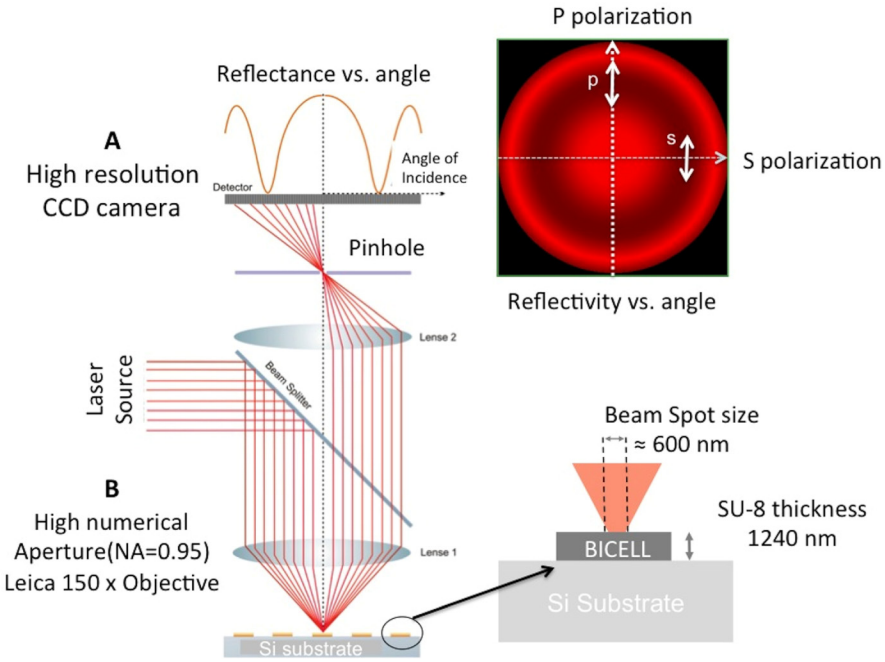

Fig. 2. Working principle of the optical technique. The angle of incidence of each of the light rays depends on the distance to the centre of the beam. The laser is lineraly polarized, and the CCD is collecting s or p polarization states depending of the orientation of the pixels. The size of the beam is in the order of 600 nm, due to the high numerical aperture objective.

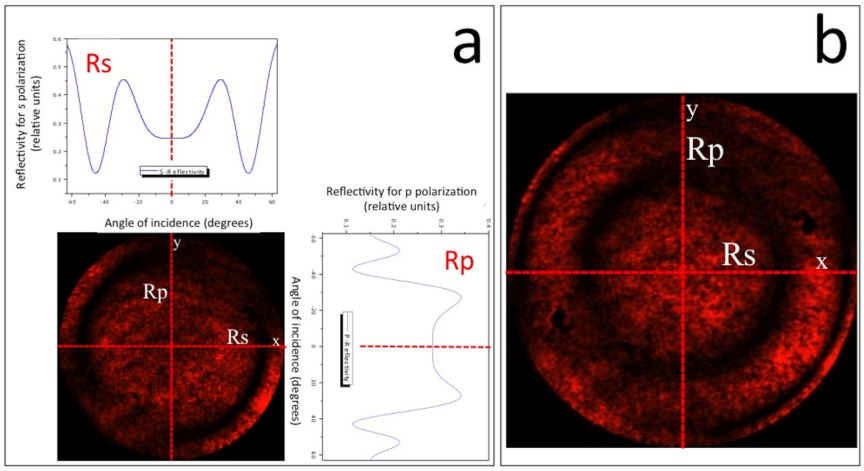

Fig. 3. Image from the high resolution CCD camera: a) interferometer of 1240 nm of SU-8 over Silicon; b) interferometer of 1770 nm of SU-8 over Silicon. Black represents zero reflectivity, and the intensity of red scale varies from zero to maximum reflectivity.

#235177 - $15.00 USD Received 24 Feb 2015; revised 27 Mar 2015; accepted 6 Apr 2015; published 4 May 2015

Instead of an array of pixels, we have used a high-resolution monochromatic CCD camera, with a total size of 2448 x 2040 pixels and a resolution in the order of 0.1°; this resolution is variable, and is higher for the angles closer to normal incidence. Each pixel in the camera is related to a particular angle of incidence, and also a particular state of polarization, depending on the position inside the beam; pixels along axis x and y pure s and pure p polarized, respectively. Figure 3 shows a couple of images from the monochromatic camera obtained for two different samples, a 1240 nm SU-8 polymer layer over a silicon substrate, and a 1770 nm SU-8 layer, again over silicon. In a) it is also shown the two pure s and p profiles for the 1240 nm sample. The range of angles of incidence covered is from −71.8° up to 71.8°.

The spectra contained along axis x and y can be renamed to Reflectivity for s polarization (Rs) and Reflectivity for p polarization (Rp). The effect of the lambda quarter plate and the polarizer can be seen in the Fig. 3 (the image would be symmetric from axis x and y without the presence of this two elements). Moreover, as seen in the figures the image given by the CCD camera is quite noisy. This kind of granular noise, known as *speckles* or *speckle noise*, is due to the high coherence of monochromatic sources, as the laser used in the experimental setup [13]. In order to reduce this noise, we have used several strategies, such as FFT filters, and Savitzky-Golay smoothing. The Rs and Rp spectra show a pattern of several interferences that can be used for sensing purposes. For example, we can track the position of the minimum placed around 47° (Rp) and 43° (Rs) as a function of the concentration of a particular bioanalyte covering the SU-8 sensing layer. Additionally to RPL, we have used FT-VIS-NIR spectrometry in order to compare results. This technique has been used previously in the characterization of BICELLs with several configurations [7].

3. Experimental results

We have fabricated several arrays of BICELLs by using UV lithography through a polymeric mask, with an experimental process described by Sanza et al. [15], but using an UV light source instead of an excimer laser for the polymerization. We fabricated four different arrays over a silicon chip of 10x10 mm, each of them containing four square BICELLs of 1x1 mm. Each of these BICELLs consists of a thin layer of SU-8 polymer acting as a resonant cavity of a vertical Fabry-Perot interferometer. This thin layer was deposited over a silicon substrate by spin coating and photopolymerized by using mask projection UV-lithography. We fabricated two different typologies of interferometers, one of 1240 and other one of 1770 nm. The optical responses can be observed in Fig. 3. In order to test the optical biosensing response, we carried out an immunoassay for the 1240 nm interferometer. For RPL, the optical measurements where collected from the centre of the BICELL and for measuring with spectrometry we employed a Hyperion microscope attached to a Bruker Vertex 70 FT-VIS-NIR spectrometer with a wavenumber resolution of 2 cm^{-1}. We employed a spot size of 1x1 mm to cover the whole BICELL previously reported in characterizing BICELLs [7,15]. Thus, the sensing areas considered for RPL and Spectrometry are not the same and may involve small differences in the immunoassay results.

The indirect immunoassay carried out consisted in immobilizing BSA as bioreceptor, and recognizing the antiBSA antibody as target. Prior to the biofunctionalization of the surface with BSA, we performed an acid catalyst of 10 seconds with 95% sulphuric acid in order to increase the hydrophilicity of the surface, as previously reported [4]. After this, we incubated a solution of 100 μg/mL of BSA in a Phosphate-Buffered Saline(PBS), during 30 min at 35°C. After this, incubation steps of increasing antiBSA concentrations where performed during 30 min at 35 °C. After each of the incubation steps, we washed the sample using deionized water and blown it with dried particle-less air to remove any unspecific bounding adsorbed onto the sensing surface. Each concentration measurement was repeated seven times. This allowed us to resolve the position of the resonances with a better accuracy and calculate the experimental uncertainty of this position.

#235177 - $15.00 USD Received 24 Feb 2015; revised 27 Mar 2015; accepted 6 Apr 2015; published 4 May 2015

3.1. Results for reflectometry

After an incubated a concentration of 100 µg/mL of BSA in PBS solution, increasing concentrations of antiBSA of 1, 2.5, 3.5, 5, 7.5, 10 and 100 µg/mL where incubated and measured. Figure 4 shows the reflectivity profiles for: a) s polarization and b) p polarization after the incubation of 100 µg/mL of antiBSA. After this step we consider that the surface is completely saturated and any biorecognition event may occur. The total shift for s polarization is of 2.38 ° and of 1.20 ° for p polarization. For removing the speckle noise, which in this typology of measurements can be significant, we studied different alternatives resulting the Savitzky-Golay filters with 50 points of window and a polynomial order of 3 as a good option. However, the speckle noise is not completely removed, particularly in those areas of the spectra from 0° to 30° of angle of incidence. Moreover, the resonances of interest are quite well defined with this filtering. The amplitude of the resonance for s polarization is clearly higher compared with p polarization; this results in a poorer filtering for p reflectivity.

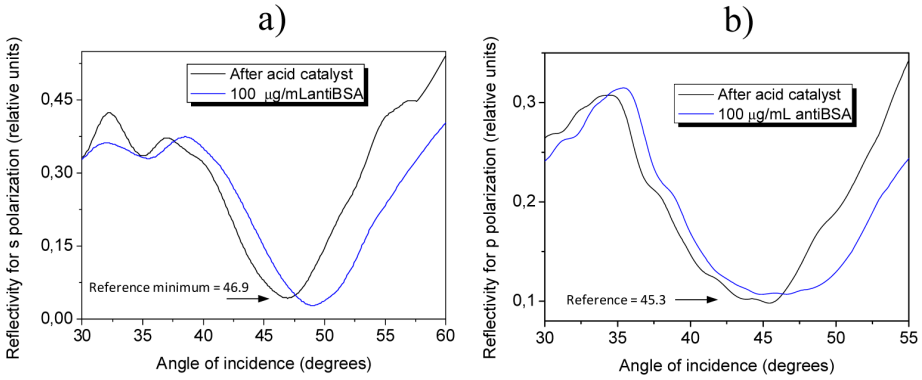

Fig. 4. Reflectivity for s polarization, for acid catalyst and 100 µg/mL of antiBSA (saturation).

Figure 5 shows the biorecognition curve of antiBSA for both s and p polarizations. The value of concentration in which the signal is reaching its half maximum is of 2.20 for Rs and 2.25 µg/mL for Rp of antiBSA.

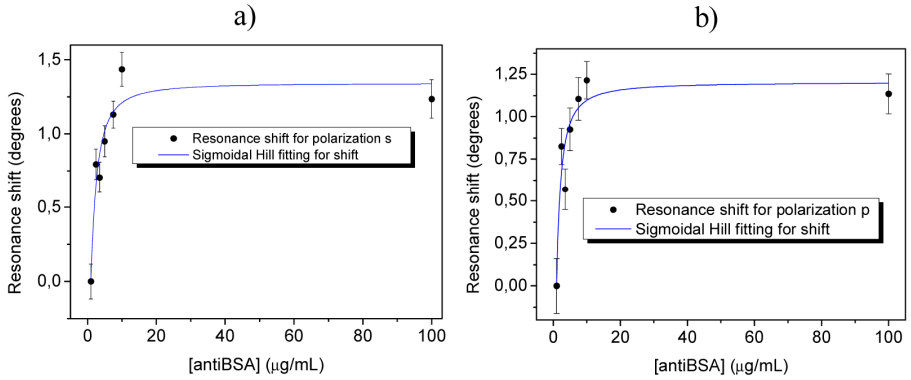

Fig. 5. Biorecognition curves for antiBSA. a) s-polarization; b) p-polarization. After immobilizing BSA, we incubated increasing concentrations of antiBSA: 2.5, 3.5, 5, 3.5, 10 and 100 µg/mL. For each concentration, we repeated the measurements seven times, we filtered the spectra using a Savitzky- Golay filter, and obtained the position of the minimum around 47 ° for the seven measurements. The graph shows the average of the seven positions.

These experimental results can be compared with the result obtained by a theoretical model. We can predict the resonance shift assuming that the complex BSA/antiBSA forms a

#235177 - $15.00 USD Received 24 Feb 2015; revised 27 Mar 2015; accepted 6 Apr 2015; published 4 May 2015

thin biofilm layer over the BICELL sensing surface, with a thickness depending on the concentration of biomolecules on the sample, but reaching a maximum thickness after the incubation of 100 µg/mL of antiBSA (there are no free BSA receptors, and thus the surface is completely saturated). This maximum thickness should be in the range of 15-20 nm, according with the size of BSA and antiBSA previously reported [7]. For obtaining the theoretical spectra, we calculated the reflectivity as a function of the angle of incidence, for an operative wavelength of 637 nm, for both polarizations, for a film stack consisting of a silicon substrate, a SU-8 layer of 1240 nm, and different thicknesses of biofilm of 0, 5, 10 and 20 nm with a refractive index of 1.4. The results are shown in Fig. 6.

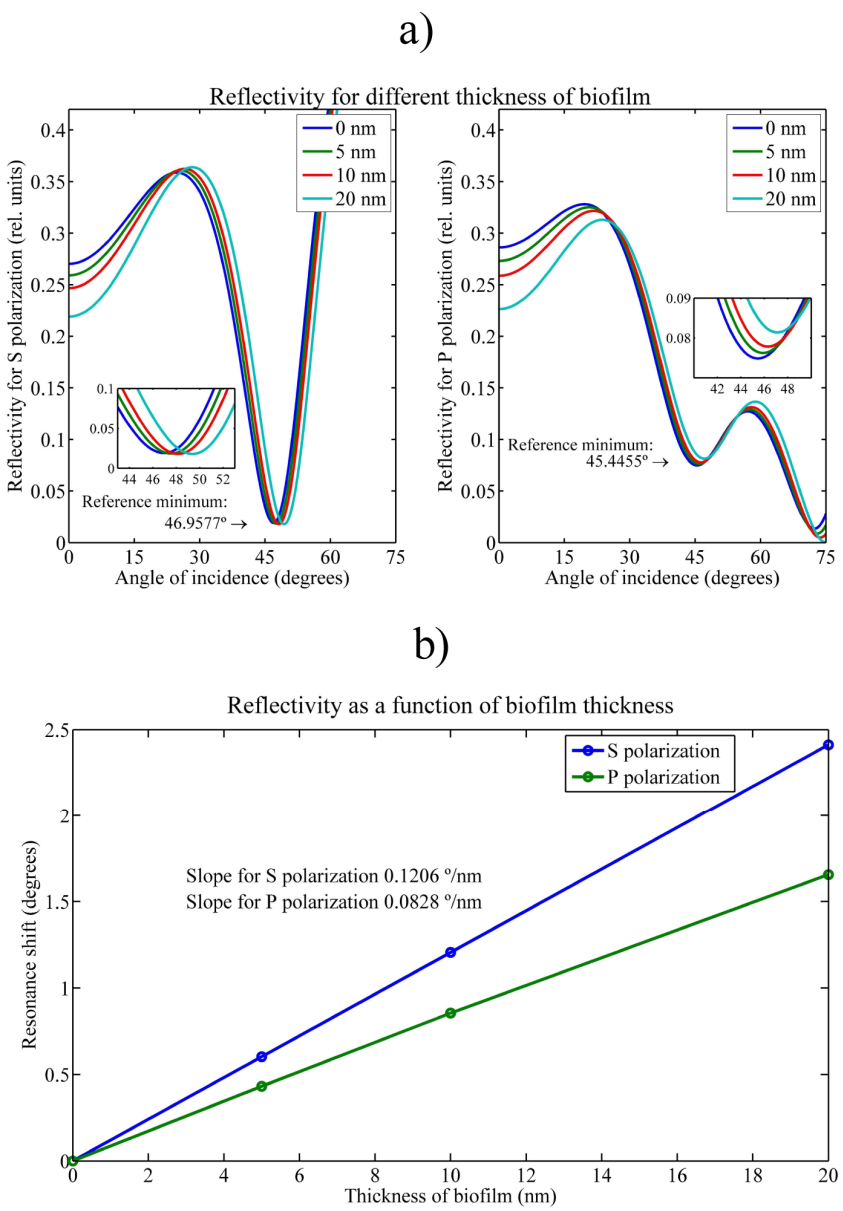

Fig. 6. Theoretical reflectivity as a function of angle of incidence. a) Reflectivity for s and p polarizations for several thicknesses of biofilm. b) Shift as a function of thickness of biofilm for s and p polarizations.

#235177 - $15.00 USD Received 24 Feb 2015; revised 27 Mar 2015; accepted 6 Apr 2015; published 4 May 2015

The experimental shift for antiBSA saturation is of 2.30° for s polarization and 1.67° for p polarization. Considering the calculation of the theoretical shift, this corresponds with an equivalent optical thickness of 19 nm of biofilm for s polarization and around 20 nm for p polarization.

3.2.Results for FT-NIR spectrometry

After the measurement of RPL profiles for each of the incubation steps, we also measured the BICELLs using Spectrometry with a spot size of 1 x1 mm (the sensing size of the whole BICELL), for all the steps of biofunctionalization and biorecognition. Figure 7 shows the reflectivity spectra after acid catalyst and after incubation of 100 µg/mL of antiBSA (surface completely saturated). We found a total shift of 7.9 nm from the beginning of the immunoassay to the total saturation of the surface. Tracking the position for dip 1 at 723 nm(see Fig. 7(a)) as a function of antiBSA concentration, results in the curve response as shown in Fig. 7(b), with a total shift of 3.24 nm for the surface completely covered with antiBSA (saturated). The value of concentration in which the signal reaches its half maximum is of 6.1 µg/mL.

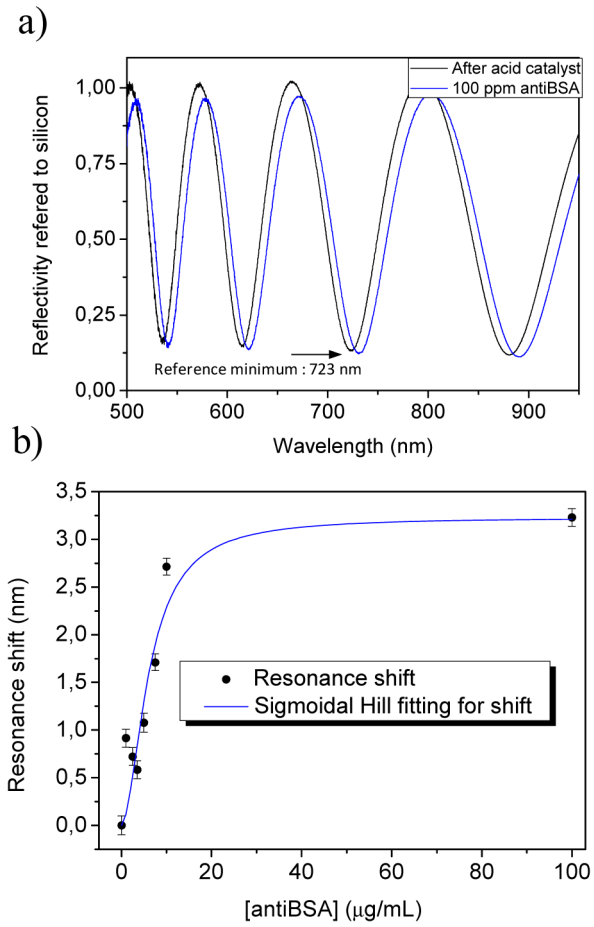

Fig. 7. FTIR spectra for reference and antiBSA saturation. After BSA inmobilization, we incubated increasing concentrations of antiBSA. We repeated the measurements seven times using the Vertex interferometer, and after filtering we obtained the average position of the minimum around 723 nm and its standard deviation.

#235177 - $15.00 USD Received 24 Feb 2015; revised 27 Mar 2015; accepted 6 Apr 2015; published 4 May 2015

The total shift for the experimental process of biofunctionalization and recognition is 7.9 nm; compared with the theoretical calculations (Fig. 8), this shift corresponds with an equivalent thickness of biofilm in the order of 20 nm (Fig. 8(b)).

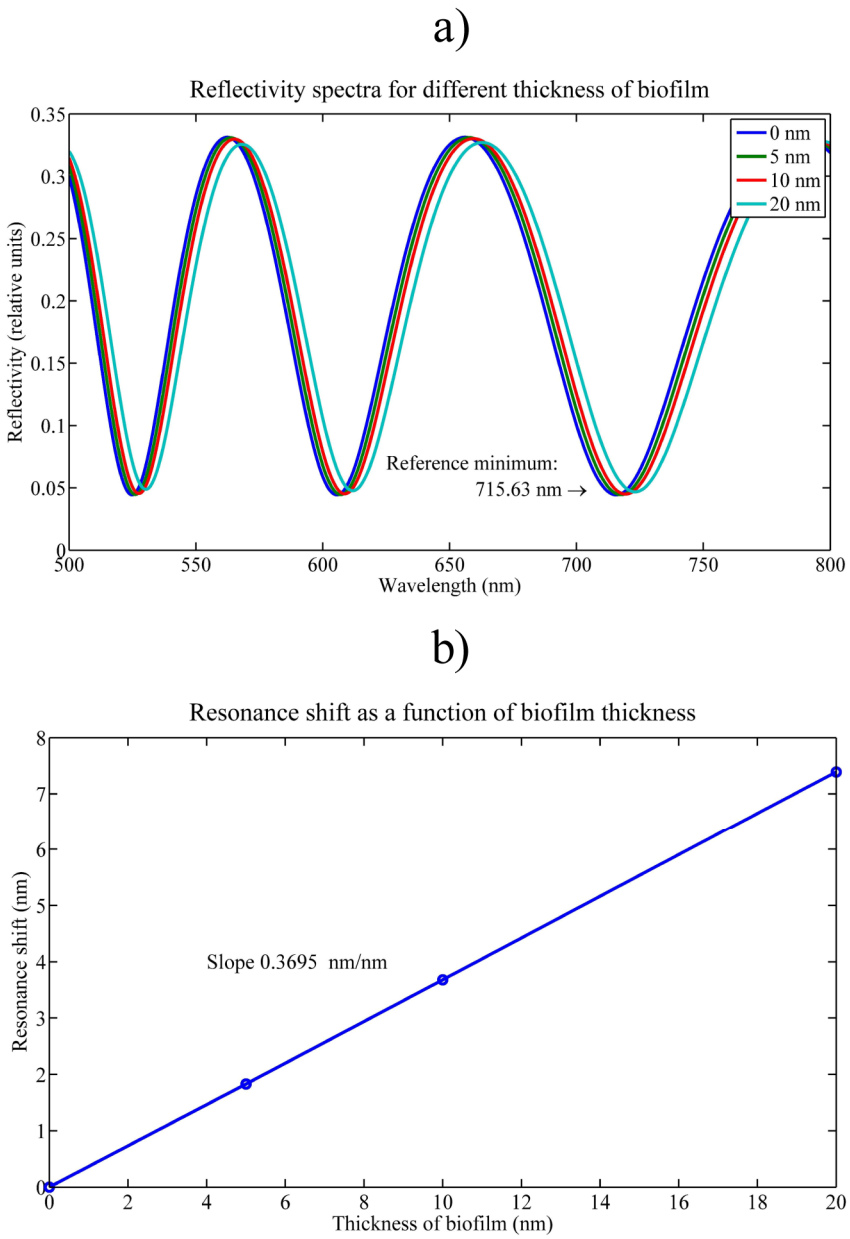

Fig. 8. Theoretical calculations for reflectometry as a function of wavelength. a) spectra for different thicknesses of biofilm. b) shift as a function of thickness of biof

3.3.Discussion of results

We can calculate the Limit of Detection (LoD) as a figure of merit to compare RPL with conventional spectrometry for the same BICELLs employed. For the calculation of the LoD of antiBSA, we have to consider Eq. (2), which is the common method used for estimating the LoD; where $U_{position}$ is the expanded uncertainty of resolving the position of the minimum

#235177 - $15.00 USD Received 24 Feb 2015; revised 27 Mar 2015; accepted 6 Apr 2015; published 4 May 2015

of the resonances, and $m_{detection}$ is the slope of the biorecognition curve in its linear range corresponding with the sensitivity of the BICELL.

$$LoD = \frac{U_{position}}{m_{detection}} \tag{2}$$

In order to calculate the expanded uncertainty of the of the resonances, which can be either for angular position (U_θ) or wavelength position (U_λ), we calculated first the standard uncertainty of the measurement following with the expression of Eq. (3), following the recommendations of the BIPM (Bureau International des Poid et Measures) in its Guide to the Expression of Uncertainty in Measurement (GUM) [16]. We have also considered a coverage factor or 3, with a probability of 99.9% and actually it is the recommended factor for In-Vitro diagnostic measurements recommended by the UIPAC. Thus, $U_{position}$ will be three times the standard uncertainty of the position. To calculate this standard uncertainty we have considered the two significant terms, the one referred to the resolution of the instrument, and another to the estimation of the standard deviation obtained for the seven measurements carried out for each concentration point measured. This is summarized in Eq. (3).

$$u^2_{position} = \frac{s^2}{n} + \frac{R^2}{12} \tag{3}$$

For the antiBSA biorecognition curves, we fitted the experimental data with a sigmoidal Hill curve; for calculating the values of $m_{detection}$ we obtained the slope of the curve at the point of half saturation, both for Reflectometry and Spectrometry measurements. For Reflectometry, the resolution of the instrument is in the order of 0.1°; the resolution of our optical setup is variable, with a minimum of 0.05° for normal incidence and a maximum of 0.13° for angles above 62°. In the range analyzed in the experiments (from 45° to 50°) the resolution is in between 0.09° and 0.1°. We have chosen a resolution of 0.1°,the maximum value in this range. For the standard deviation of the position of the minimum we have calculated the average of the deviation for the measurements for the eight different antiBSA concentrations. For s polarization, this gives a value for $m_{detection}$ of 0.353 °/(μg/mL), and a value for the standard deviation of 0.109°; this results in an expanded uncertainty of 0.151° and a value of LoD of 427.76 ng/mL. For p polarization, $m_{detection}$ has a value of 0.295 °/(μg/mL), the standard deviation is 0.124°; thus the expanded uncertainty equals to 0.165°; resulting in a LoD of 559.32 ng/mL. The value of LoD was expected to be poorer in p polarization since the amplitude of the resonance is lower compared with Rs, with the same level of speckle noise. For Spectrometry, the value of $m_{detection}$ is of 0.3 nm/(μg/mL), with a standard deviation of 0.093 nm and an expanded uncertainty of 0.131 (for a resolution of the instrument of 0.09 nm at 723 nm). We reported, in a previous work [7] a limit of detection of 2.3 ng/ mL for FTIR spectrometry in a SU-8 nanopillars based system, but considering the optimal resolution for the instrument (0.1 cm^{-1}) and neglecting the effect of the standard deviation of the measurements in the uncertainty of the measurement. Ho and associates [17], reported a biosensor based on SPR phase difference, with a LoD of 7.4 ng/mL, but also considering an optimal resolution of the system (0.01°). If we calculate our limit of detection consdering only the optimal angle resolution reachable (that could be in the order of 0.01°), this limit of detection could be estimated in the order of 28 ng/mL.

The results are in good correlation with theoretical calculations; the equivalent thickness optically calculated for reflectometry is of 19 nm for s-polarized reflectometry, and 20 nm for p- polarized reflectometry and for spectrometry. This is in the range of 15-20 nm that we have found in previous works [7,13].

4. Conclusions

We have described the application of a reflectometry based technique (RPL) for label free biosensing purposes. This technique have several remarkable aspects: the sub-micrometric

#235177 - $15.00 USD Received 24 Feb 2015; revised 27 Mar 2015; accepted 6 Apr 2015; published 4 May 2015

spot size achieved, the possibility of collecting reflectivity as a function of multiple states of polarization with an angular resolution of 0.1 °, allowing to characterize reduced areas with high sensibility, which can be interesting in highly integrated systems with reduced sensing area, or when the amount of analyte to be measured is reduced. An immunoassay is performed over a SU-8 sensing cell, both with RPL and a previously studied technique (FT-VIS-NIR) and used in the biorecognition of several analytes. Although it is not the objective for this paper to achieve the best LoD, which depend of sensitivity of the BICELLs employed as transducer, what we consider remarkable is that the results exhibits for both techniques the same order of magnitude in LoD (427.76 ng/mL, for Reflectometry polarization s, and 436.66 ng/mL for Spectrometry), but with the advantage for RPL to evaluate sub-micrometric domains for immunoassays reactions onto a sensing surface.

Acknowledgements

This work has been partially funded under the projects under the projects PLATON (Ref: TEC2012-31145) and INNBIOD (Ref: IPT-2011-1429-01000) from the Ministerio de Economía y Competitividad (MINECO) of Spain. We acknowledge Nightingale-EOS and Stephen Morris for his contribution to the development of this optical tool.

#235177 - $15.00 USD Received 24 Feb 2015; revised 27 Mar 2015; accepted 6 Apr 2015; published 4 May 2015